

SHORTCIRCUIT: ALPHAZERO-DRIVEN CIRCUIT DESIGN

**Dimitrios Tsaras^{1,2}, Antoine Grosnit^{1,3},
 Lei Chen¹, Zhiyao Xie²,
 Haitham Bou-Ammar^{*1,4}, Mingxuan Yuan^{*1}**
 Noah’s Ark Lab, Huawei¹, HKUST², TU Darmstadt³, University College London⁴

ABSTRACT

Chip design relies heavily on generating Boolean circuits, such as AND-Inverter Graphs (AIGs), from functional descriptions like truth tables. While recent advances in deep learning have aimed to accelerate circuit design, these efforts have mostly focused on tasks other than synthesis, and traditional heuristic methods have plateaued. In this paper, we introduce ShortCircuit, a novel transformer-based architecture that leverages the structural properties of AIGs and performs efficient space exploration. Contrary to prior approaches attempting end-to-end generation of logic circuits using deep networks, ShortCircuit employs a two-phase process combining supervised with reinforcement learning to enhance generalization to unseen truth tables. We also propose an AlphaZero variant to handle the double exponentially large state space and the sparsity of the rewards, enabling the discovery of near-optimal designs. To evaluate the generative performance of our trained model, we extract 500 truth tables from a benchmark set of 20 real-world circuits. ShortCircuit successfully generates AIGs for 84.6% of the 8-input test truth tables, and outperforms the state-of-the-art logic synthesis tool, ABC, by 14.61% in terms of circuits size.

1 INTRODUCTION

The rapid proliferation of AI has triggered an unprecedented surge in computational demands, exceeding the capabilities of existing hardware and thereby becoming a major bottleneck to AI’s continued growth. To enable further advancements in AI and other domains, the development of new hardware is crucial. Chip design plays a pivotal role in this development effort allowing the next-generation of computing systems to emerge. However, traditional methodologies struggle to keep pace with the accelerating demands, underscoring the need for innovative approaches to accelerate the design process and discover novel architectures.

At its core, a chip is the physical embodiment of a Boolean function, transforming binary inputs into desired outputs. The creation of these Boolean functions is facilitated through logic synthesis, a crucial step in chip design that converts high-level functional descriptions into Directed Acyclic Graphs (DAGs) comprising logic gates. The resulting circuit must balance competing objectives, including power efficiency, performance, and silicon area (PPA), presenting a formidable optimization challenge. In this paper, we investigate the potential use of Machine Learning (ML) to generate optimized digital circuits directly from Boolean logic specifications, offering a fresh perspective on the chip design process.

A fundamental way to describe a Boolean function is to represent it as a truth table, i.e., exhaustively enumerating the output values for all possible binary input combinations. We adopt truth tables as the input Boolean logic description for our problem, as they provide a complete and unambiguous representation of the desired functionality. The output of our approach is a directed acyclic graph (DAG) in the form of an AND-Inverter Graph (AIG), a widely used data structure in Electronic Design Automation (EDA) (Mishchenko and Brayton, 2006; Wolf et al., 2013; Mishchenko et al., 2007). AIGs consist of 2-input AND-gates as nodes, connected with normal or inverted wires,

*Equal supervision

offering a simple, scalable, and universal intermediate representation for various EDA applications. Their popularity in the industry stems from their ability to efficiently represent complex Boolean functions, making them an ideal choice for our ML-based circuit generation approach.

Recent efforts attempt to accelerate chip production by leveraging the development of ML methods at the different steps of EDA (Beerel and Pedram, 2018; Huang et al., 2021; Gubbi et al., 2022), notably for placement (Ward et al., 2012a;b), routing (Xie et al., 2018; Alawieh et al., 2020), verification (Fine and Ziv, 2003; Wagner et al., 2007), and for logic synthesis (Tu et al., 2024; Haaswijk et al., 2018a). Rather than directly tackling the graph generation problem, most ML methods for logic synthesis focus on the optimization of synthesis recipes. These recipes are sequences of operators that act on a logic graph (e.g., an AIG) to modify its topology, while preserving the underlying boolean function this graph represents. Various methods ranging from CNN-based classification (Yu et al., 2018), Reinforcement learning Hosny et al. (2020); Haaswijk et al. (2018a); Yuan et al. (2023); Zhu et al. (2020a); Qian et al. (2024); Chowdhury et al. (2024), Monte Carlo Tree Search (Pei et al., 2023), or Bayesian optimization (Grosnit et al., 2022; Feng et al., 2022) have been developed to tune the sequence of logic operators to get the best possible PPA. More recently, deep-generative methods emerged aiming to generate logic graphs rather than sequences of graph operators d’Ascoli et al. (2024); Li et al. (2024a;b); Lai et al. (2024); Dong et al. (2023). The generative approach offers higher potential as it offers more flexibility than working with a fixed set of operators; on the other hand, this approach involves exploring a much larger space.

Generating AIGs poses significant challenges, primarily due to the double exponential growth of the search space with the number of Boolean function inputs. This vast search space renders traditional ML methods ineffective for optimal AIG generation. However, recent advances have demonstrated that, with tailored model architectures and exploration-exploitation-aware training protocols, remarkable performance can be achieved even in tasks involving such large spaces. Indeed, we can attribute the success of methods like AlphaGO Silver et al. (2016), AlphaZero Silver et al. (2017), AlphaFold Jumper et al. (2021) and even the emergence of large language models Devlin et al. (2019); Kaplan et al. (2020); Brown et al. (2020) to the development of customized model architectures capturing structural properties of board games, proteins, or natural language. Moreover, the training of these models either leverages naturally abundant data or employs specific data-augmentation and exploration-exploitation strategies to improve their performance.

In this work, we propose ShortCircuit, a new transformer architecture structurally adapted for generating AND-Inverter graphs. Our transformer takes logic nodes represented as truth tables as input, and each forward pass predicts the next AND node to create in order to realize a target truth table. Moreover, we utilize an AlphaZero policy variant to effectively navigate the large state space and discover more compact designs. Our contributions are summarized as follows:

- We formally define the challenging problem of generating And-Inverter Graphs (AIGs) from target truth tables, characterized by a doubly exponential state space and a quadratically expanding action space.
- We introduce ShortCircuit, a novel transformer-based architecture that incorporates structural awareness of AIGs and the underlying Boolean logic, enabling effective exploration of the vast search space.
- We propose a two-step training approach, combining supervised learning and reinforcement learning, to efficiently learn generalizable patterns and prune the search space, improving solution quality and scalability.
- Through extensive experiments, we demonstrate the effectiveness of ShortCircuit by producing circuits that are 14.61% smaller compared to the state-of-the-art logic synthesis tool ABC (Mishchenko et al., 2007), and showcase the potential of machine learning methods to revitalize the field of logic synthesis with a fresh perspective.

We organize the rest of the paper as follows. Section 2 introduces the necessary concepts and related works, providing a grounding for the formal problem formulation that we present in section 3. We then detail our proposed approach, notably our model architecture 4 and our tailored training procedure in section 5. We finally present in section 6 an empirical evaluation of our method’s performance.

corresponds to the values of the AIG nodes for a specific set of entries $(I_1, I_2, I_3) = (i_1, i_2, i_3) \in \{0, 1\}^3$ displayed on the left part of the table. We can extract from this representation a binary vector of size 2^3 (in general 2^n) for each node of the AIG. For instance, the vector representation, or by abuse of notation the “truth table”, of node \wedge_4 is $(0\ 0\ 0\ 1\ 0\ 0\ 0\ 1)^\top$, and the truth table of the primary output is $(1\ 1\ 1\ 1\ 0\ 0\ 0\ 1)^\top$.

After discussing related works in more details, we will explain in the next section how our method utilizes this rich vector representation to learn how to generate AIGs.

2.3 RELATED WORKS

Heuristics for AIG generation and optimization As the derivation or inference of CNFs using exact SAT solvers often lead to exponentially large expressions, various heuristics (Karnaugh, 1953), methods (Quine, 1952; 1955; McCluskey Jr., 1956), and algorithms (Rudell and Sangiovanni-Vincentelli, 1987) have been designed to obtain more compact expressions or circuits. Further efforts accompanying the rise in chip demand led to the development of widely used logic synthesis libraries implementing equivalence-preserving boolean network operators. The open-source library ABC (Mishchenko et al., 2007) notably comprises dozens of logic graph operators aiming at reducing a network size or depth (Mishchenko et al., 2011; Mishchenko and Brayton, 2006). Interestingly, some important operators such as `resub` or `rewrite` (Darringer et al., 1981; Mishchenko et al., 2006) acts on the subject graph through a series of local modifications involving reasonably small single-output AIGs. Besides, applying a single operator on a logic network is suboptimal compared to applying several operators sequentially, though finding the best sequence is also a hard problem (Riener et al., 2019).

Machine learning for logic synthesis Many ML approaches have been explored to tackle the operator flow optimization progress. Some stateless optimization methods, such as Bayesian optimization (Grosnit et al., 2022; Feng et al., 2022), search for the best flow without considering the specificities of the subject graph. Alternatively, state-based methods formulate the operator sequence optimization as a Reinforcement learning problem, and train policies on selected features of the logic network. While some works use high-level statistics of the subject graph (e.g., its number of nodes) (Hosny et al., 2020; Zhou and Anderson, 2023; Qian et al., 2024), others rely on tailored Graph Convolutional networks (GCN) to extract richer features at the cost of a longer training time (Haaswijk et al., 2018b; Zhu et al., 2020b; Peruvemba et al., 2021; Basak Chowdhury et al., 2023). Similarly, standard deep network architectures, such as convolutional neural networks (Yu et al., 2018), LSTM (Yu and Zhou, 2020), or GCN (Wu et al., 2022) have been trained to predict the quality of a logic synthesis flow in a supervised way. Contrary to these works, we target the AIG generation itself and not the operator optimization.

Deep Generative Models for circuit design One approach to generate Boolean networks with deep neural networks consists of substituting the gates and wires of a logic circuit by learnable nodes and connections forming a neural network (Belcak and Wattenhofer, 2022; Zimmer et al., 2023; Hillier et al., 2023). The parameters of the network are learnt by minimizing the difference between the ground truth binary output and the result of a forward pass for each combination of input values. The main advantage of this method is that it can cope with larger number of primary inputs, and work for different types of digital circuits, as instead of learning an entire family of logic graphs (e.g., the 8-input AIGs), it is specialized on one particular target truth table. However, this means that a new neural network must be trained for each target truth table, representing a significant runtime bottleneck.

Therefore, several works inspired by the development of foundational generative models have followed another direction, consisting in learning synthesis process itself with a deep neural network. While Roy et al. (2021) use a CNN backbone to specifically generate prefix circuits adding or deleting nodes in a $N \times N$ grid, Li et al. (2024c) employ an auto-regressive diffusion model to generate DAG for high-level synthesis (HLS) stage, and Dong et al. (2023) design a two-level GNN architecture to synthesize analog circuits that work with non-binary signals. The closest related works are Boolformer (d’Ascoli et al., 2024) and “Circuit Transformer” (Li et al., 2024a), both tackling synthesis of digital networks with an auto-regressive transformer-based architecture. They train their policies with a supervised training phase, predicting the next element of a logic graph given a target

truth table, and doing inference through beam-search or Monte Carlo Tree Search (MCTS) simulations. Contrary to our work, Boolformer and Circuit Transformer use a symbolic representation of the Boolean formula associated to a logic graph that they encode via depth-first search. Therefore instead of representing already built nodes by their truth tables and predicting the next node to add to the graph, they tokenize the symbols and let their model generate the next symbol of the logic formula (a logical operation, an input or an output), which requires more forward passes than for our method to produce a similar AIG. Besides, given a target truth table T_* , Boolformer directly takes as input the boolean representation of T_* as we do, Li et al. (2024a) pass a (non-optimal) AIG realizing T_* to its Circuit Transformer to generate an improved logic network.

We show in the next section how we can adapt the transformer architecture to perform next-gate prediction in AIG synthesis.

3 PROBLEM DEFINITION

Computing the truth table of the output node O of a given AIG, as shown in Section 2, is straightforward, but deriving an AIG from a given truth table is not trivial. Even though a truth table encompasses the results for all possible input values, it does not provide sufficient structural information to derive an AIG with the corresponding output representation. Heuristics developed to generate a CNF, or equivalently an AIG, from a truth table generally lead to exponentially large solutions that need further refinement. Consequently, solving this AIG generation problem would significantly impact digital circuit design.

Problem Definition: Given a target truth table $T_* \in \{0, 1\}^n$, construct an AIG with the minimum number of nodes, such that its output node O has a truth table T_O that matches T_* .

One of the main difficulties of this problem arises from the double exponential growth rate of the search space with respect to the number of primary inputs. Indeed, the size of a truth table associated with an n -input AIG is 2^n . Thus, the set containing all truth tables of size 2^n has a cardinality of 2^{2^n} . For instance, the truth tables that a 6-input AIG can represent belong to a state space with a magnitude of 10^{191} . Exploring such a large space efficiently requires developing specific models and training techniques. These must exploit the structural properties of the problem while managing the exploration-exploitation trade-off inherent in such scenarios.

3.1 STATE REPRESENTATION & NOTATIONS

We formally define an AIG with n inputs as a graph $\mathcal{G} = (V, E)$, where V and E represent the node and edge sets, respectively. To capture the dynamic nature of AIG construction, we introduce a temporal parameter t , which simultaneously represents the current time step and the number of AND-nodes in the graph, denoted as $\mathcal{G}_t = (V_t, E_t)$. This allows us to model the evolution of the AIG over time, with the graph growing as new AND-nodes are added. We assign a unique integer ID to each node in the graph, regardless of its type; thus, at time t the node set is $V_t = \{I_1, \dots, I_n, \wedge_{n+1}, \dots, \wedge_{n+t}\}$, or with a node-type agnostic notation $V_t = \{v_1, \dots, v_{n+t}\}$. Following this notation, the graph \mathcal{G}_0 represents an AIG containing only input nodes, i.e., with $V_0 = \{I_1, I_2, \dots, I_n\}$.

In our generative process, the state corresponding to AIG \mathcal{G}_t is encoded as a 3-tuple $s_t = (\mathcal{T}_t, T_*, \mathcal{A}_t)$. Here, $\mathcal{T}_t = \{T_1, T_2, \dots, T_{n+t}\}$ is the set of truth tables associated with the current nodes, T_* is the target truth table, and $\mathcal{A}_t = \{a_{n+1}, a_{n+2}, \dots, a_{n+t}\}$ is the ordered set of actions performed so far. Each action generates a new AND-node by connecting two existing nodes in one of four possible configurations: (v_i, v_j) , $(v_i, \neg v_j)$, $(\neg v_i, v_j)$, and $(\neg v_i, \neg v_j)$. Our objective is to perform a series of N actions, transforming \mathcal{G}_0 into a terminal AIG \mathcal{G}_N such that the truth table of the last generated AND-node, T_{n+N} , matches or is the negation of the target truth table T_* . A notable aspect of our environment is its statefulness, meaning that its history influences future decisions. Furthermore, our environment poses an additional challenge due to its action space expanding quadratically with each new node we add.

¹Or a magnitude of 10^{16} if we account for permutations of primary inputs.

4 METHOD

We propose an iterative approach to AIG construction, where we gradually build the circuit, ensuring its functionality at each step. Initially, the graph contains only the input nodes, and at each step, we let the model decide which nodes of the graph to combine through an AND gate to produce a new node. We can straightforwardly compute the truth table of the new node from the truth tables of its parent nodes and of the edge type. The goal of the model is to combine the nodes such that it eventually produces the expected output node matching the target truth table. To generate the next gate, the model takes the set of existing nodes as input, and it outputs a probability distribution over the set of nodes that can be built by combining any pair of already existing nodes, considering the edge types.

Formally, let $|V_t|$ denote the number of nodes in the current state of the graph, then the action space is a $4 \times |V_t| \times |V_t|$ tensor, where each $|V_t| \times |V_t|$ slice correspond to a connection type. Specifically, the cell (i, j) in a given slice indicates the probability of connecting node v_i with v_j , and the slice index, in $\{1, 2, 3, 4\}$, corresponds to a combination of specific edge types: (v_i, v_j) , $(\neg v_i, v_j)$, $(v_i, \neg v_j)$, or $(\neg v_i, \neg v_j)$, respectively. Therefore, we can sample a triplet (ϵ, i, j) following the distribution given by this $4 \times |V_t| \times |V_t|$ tensor and add the corresponding node to the graph. The process ends when the truth table of the sampled node matches the target truth table (up to full negation) or after a maximum number of steps N_{\max} is reached.

4.1 MODEL ARCHITECTURE

To effectively explore and prune the vast state space, the model utilizes AlphaZero Silver et al. (2017) to assess intermediate states and strategically get closer to the desired target. The model architecture consists of a common core where position encodings are applied to the truth tables, followed by H many transformer encoder layers. Then, the hidden embeddings are passed as input to the 4 stacked policy modules and to the value module. The stacked policy modules followed by a softmax layer produce the action probabilities and the value module with tanh layer guesses

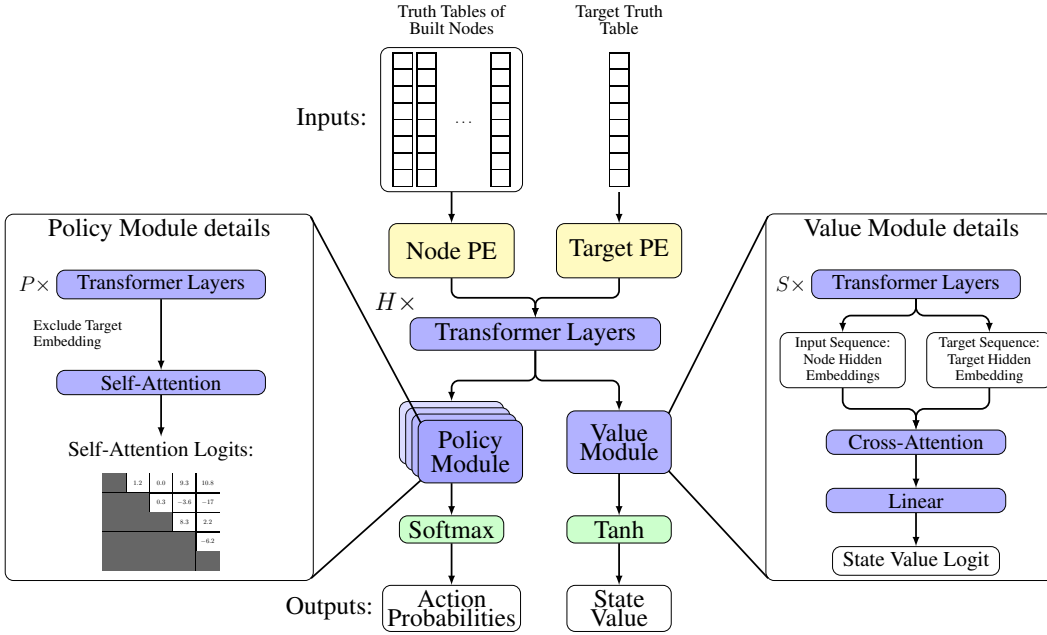


Figure 2: Model architecture based on transformers. It takes as inputs the truth tables of the nodes that are already built and the target truth table, and it appends a positional encoding that depends on the node type. After going through several transformer layers, the model is split into two heads respectively outputting a probability distribution over the next possible actions (policy module on the left), and a value that should reflect the quality of the current inputs (value module on the right).

the expected reward in $[-1, 1]$. To preserve the auto-regressive property we apply a causal mask specifically geared towards this problem.

4.1.1 POSITIONAL ENCODING

Positional encoding allows the model to capture a sequential relation in the inputs. If a transformer model does not apply any positional encoding to its inputs, it simply maps a set to another set, since inputs with the same embeddings are indistinguishable in the self-attention computation. In our setting, we do not need to hint the model about the structure of the graph, as the truth tables already convey all the necessary information. Additionally, the self-attention operation should treat every node equally, as there is no limitation at any stage regarding which two nodes can be combined to form a new node. Nevertheless, the model should be able to treat differently the nodes in the AIG it is building and the target node. As no standard positional encoding exists for this specific use case, and since we only need to distinguish those two types of nodes, we introduce only two learnable positional encoders (“Node PE” on Figure 2).

4.1.2 POLICY MODULE

Transformers are the state-of-the-art architecture to handle sequential data. These models particularly shine when trained to predict the next token in a sequence. Instead of directly generating the next token, a transformer usually outputs a fixed-size tensor representing the probabilities of choosing each element of a token glossary as the next token. In our case though, the set of nodes that we can add to an AIG is growing at each step, as more pairs of nodes can be combined to produce the next node. Inspired by natural language processing (NLP) tasks, for which attention scores among related tokens are high, we use attention to guide next node generation. Thus, we directly use the final self-attention map of four parallel policy modules to get the probability to connect any two nodes with specific edge types.

Each policy module has P transformer encoder layers and a final self-attention layer. In the last self-attention layer, we exclude the entry corresponding to the target node and returns the self-attention scores based on the existing AIG nodes embeddings. We aggregate the scores from the four policy modules and mask the ones associated to building nodes that are already built in the current AIG (up to negation). We finally apply a softmax to the remaining scores to produce a single probability distribution.

4.1.3 VALUE MODULE

The value module is a critical component to assess how favorable a state is and therefore prevent expanding unpromising states. Our value module consists of S many transformer encoder layers. As the quality of a state not only depends on the nodes that are present in the graph at that stage, but also on the target truth table that should be realised, the value module also uses the two learnable type-based positional encoders introduced above. After performing the embedding, we compute the cross-attention between the graph nodes and the target truth table, which yields a new vector representation of the target. Finally, we feed this vector to a linear layer producing a single value, which should reflect the quality of the current state.

5 TRAINING SHORTCIRCUIT

The sparse nature of the problem r makes it practically impossible to discover functionally correct graphs when exploring the double exponential state space uniformly. This challenge necessitates a more effective training approach for our ShortCircuit. To address this, we propose a two-stage training regimen consisting of a supervised pre-training stage to initialize the policy module, followed by an AlphaZero-style fine-tuning phase to improve the policy module and train the value module. Although pre-training the policy module provides a good prior to predict the most useful next actions, simply following it does not guarantee that an AIG matching T_* will be constructed due to the inherent difficulty of the problem. This limitation highlights the importance of the fine-tuning stage, which aims to refine the policy module and leverage the value module for improved performance.

5.1 PRE-TRAINING

Just as large language models in NLP are pre-trained using next-token prediction, we can pre-train our transformer model on a next-node prediction task. This approach requires a corpus of single-output AIGs that our model can learn to regenerate node by node, starting with only the truth tables of the primary inputs and the target T_* . Since the AIG generation problem has not been previously addressed by the ML community, there is no large, well-structured corpus of publicly available (truth table, AIG) pairs to perform this pre-training. However, we can curate a dataset of single-output AIGs for the pre-training of ShortCircuit by leveraging existing open-source collections of digital circuits.

5.1.1 DATA EXTRACTION

To generate an AIG dataset with the desired input and output sizes, we utilize the EPFL benchmarks (Amarú et al., 2015), which contain a collection of 20 real circuits: 10 arithmetic and 10 random control circuits. On average, the arithmetic circuits have 17 inputs, 10 outputs, and 37,000 nodes per circuit, while the random control circuits have 28 inputs, 18 outputs, and 7,600 nodes. Since these circuits have more inputs than the AIGs we aim to generate, we extract subgraphs, or *cuts*, from them.

A cut refers to a connected subset of nodes in the AIG that divides the graph into two disjoint parts. The root node of a cut is the node to which all directed paths within the cut converge and a *leaf node* is a node in the cut that have at least one fanin outside of the cut. By design, there is no path from a primary input to the root node that does not pass by a leaf node, and the cut itself forms a single-output AIG with a number of inputs corresponding to the number of leaves. We defer to Appendix B.2 the full description of the cut extraction method we develop to build a dataset of single-output AIGs.

5.1.2 DATA PREPARATION

We can train our policy network to generate the AIGs we have in our dataset in a supervised way. Since our policy should predict the next action, i.e. the next node to add to a partial AIG, we need to convert the AIGs we load from our training dataset into a sequence of actions. As different series of actions can lead to the same graph with N nodes, we first sort the nodes of the training AIG we load into a valid topological order $\{I_1, \dots, I_n, \wedge_{n+1}, \dots, \wedge_N\}$ (or $\{v_1, \dots, v_N\}$ with node-type agnostic notation), where \wedge_N is connected to the output O . We also convert the AIG nodes into truth tables, as described in section 2, and use the truth table of its primary output O as the target truth table T_* . From the topological sequence of AIG nodes, we build the sequence of actions that our policy should learn to perform when being given T_* as input. As mentioned in section 4, we represent the creation the node $v_i = (\neg)v_{p_1} \wedge (\neg)v_{p_2}$, with $1 \leq p_1 < p_2 < i$, by the action $a_i = (\epsilon, p_1, p_2)$. The first component of a_i , that is $\epsilon \in \{1, 2, 3, 4\}$, indicates the types of the edges connecting v_i to its parents, as detailed in Table 2. This procedure leaves us with the sequence of actions $\mathcal{A} = \{a_{n+1}, a_{n+2}, \dots, a_N\}$. Note that the first action has index $n + 1$ since the n primary inputs are given at the beginning of the AIG generation process.

ϵ	Build \wedge_i from (ϵ, p_1, p_2)
1	$\wedge_{p_1} \wedge \wedge_{p_2}$
2	$\neg \wedge_{p_1} \wedge \wedge_{p_2}$
3	$\wedge_{p_1} \wedge \neg \wedge_{p_2}$
4	$\neg \wedge_{p_1} \wedge \neg \wedge_{p_2}$

Table 2: Connection types for each value of ϵ .

To efficiently generate target action distributions, we aggregate all the actions into a sparse 3-dimensional tensor $\mathbf{A} = (\mathbf{A}_1, \mathbf{A}_2, \mathbf{A}_3, \mathbf{A}_4)$ where each element \mathbf{A}_ϵ is a $N \times N$ matrix representing the actions with connection type ϵ . The value of the entry (p_1, p_2) of \mathbf{A}_ϵ is set to 1 if (ϵ, p_1, p_2) belongs to \mathcal{A} and to zero otherwise. Thus, if all the nodes up to v_i are already built, considering each submatrix $\mathbf{A}_{\epsilon, 1:i, 1:i}$ taking the first i rows and i columns of \mathbf{A}_ϵ allows to easily identify which nodes with connection ϵ we could build next. Taking the submatrices for all values of ϵ , we obtain the target action distribution by setting the entries corresponding to already performed actions at 0, and normalizing the resulting tensor. Figure 3 shows how we build the action tensor from a raw AIG coming from our training set.

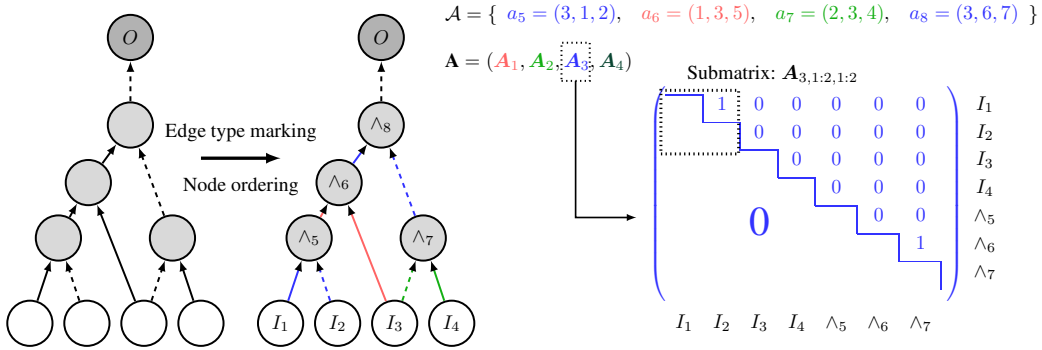


Figure 3: Data pre-processing. The AIG on the left is fort sorted in topological order, starting from its primary inputs. The type of actions $\epsilon \in \{1, 2, 3, 4\}$ depends on the nature of the incoming edges. Once the nodes are sorted and the action type identified, we build the sequence of actions \mathcal{A} , shown on the right, and generate the global action tensor $\mathbf{A} = (\mathbf{A}_1, \mathbf{A}_2, \mathbf{A}_3, \mathbf{A}_4)$. We notably present the structure of \mathbf{A}_3 which contains a 1 at entry (1, 2) and (6, 7) associated to the generation of \wedge_5 (action a_5) and of \wedge_8 (action a_8).

5.1.3 DATA AUGMENTATIONS

The first data augmentation we employ involves using the same AIG for both targets T_* and $\neg T_*$. This is valid because we can generate one target or the other by connecting the final node \wedge_N with the output O using either a regular or an inverter edge. The second data augmentation method leverages the fact that any order of the rows in the truth tables is valid, provided that we keep the same order for all the nodes at any given step. Since our model’s inputs are truth tables, it is desirable for the model to be invariant to row permutations. Formally, the model should generate the same next-action prediction whether we give it as input the truth tables T_1, T_2, \dots, T_N and T_* , where $T_i = (t_i^{(1)}, \dots, t_i^{(2^n)}) \in \{0, 1\}^{2^n}$, or when we give it the permuted truth tables $\sigma(T_1), \sigma(T_2), \dots, \sigma(T_N), \sigma(T_*)$ where σ is a permutation in \mathbb{S}_{2^n} and $\sigma(T_i) = (t_i^{(\sigma(1))}, \dots, t_i^{(\sigma(2^n))})$. Structurally encoding this invariance into our policy architecture would be computationally too expensive. Instead, We sample random permutations that we apply to the inputs of our model during the training. We can efficiently apply this without affecting any of the other metadata we introduced in the previous section.

5.1.4 PRE-TRAINING FLOW

With the data prepared, we can proceed to train our model. As depicted in Figure 2, the backbone of our model is a transformer. To maintain the causality in the auto-regressive generation process, we implement a custom masking strategy during training. Since the primary inputs and the target truth table are available from the start, and as there is no causality for their existence, we allow full attention for their embeddings, and only apply a causal mask for the rest of the nodes.

The policy module’s objective is to learn how to recommend the correct actions to generate the desired target. Instead of framing this as a multi-label classification problem, we treat the policy output as a probability distribution. This approach is more appropriate since we need to select the most optimal action rather than evaluating each “label” independently. For training loss, we experimented with KL divergence and cross-entropy, both of which measure the distance between two probability distributions. In practice, KL divergence loss yielded better results.

5.2 FINE-TUNING

Fine-tuning aims to align the policy module and value module so they operate effectively together. We can view the policy module as a compass suggesting valid actions and the value module as an observer evaluating the quality of the position, indicating whether the current state of the graph is close or drifting away from reaching the target truth table. The policy module alone can propose actions, but it lacks the ability to gauge how close the current graph state is to achieving the target

truth table. As mentioned in Section 4.1.3, this is where the value module comes into play, predicting a “goodness” score for each state relative to the target. This score represents the expected reward at the end of the trajectory.

Unlike the policy module, the value module cannot be properly initialized during pre-training, because the generated dataset only contains successful examples. Consequently, the value module would only encounter “good” states and might incorrectly evaluate unseen states as being equally good. On the other hand, skipping pre-training is not an option either, as exploring the vast search space of truth tables with random actions would likely result in encountering only “bad” states, preventing the model from learning what constitutes a “good” state. While artificially creating “bad” states could be a potential strategy, it is difficult to estimate their actual distance from the target. Therefore, the most effective way to train our value module is through experience, by performing searches with an initialized policy module. We utilize AlphaZero as the orchestration framework to refine the policy and value modules.

5.2.1 ALPHAZERO

AlphaZero has demonstrated remarkable success in board games with enormous state spaces, such as chess (10^{44}) and Go (10^{170}) (Silver et al., 2017). Since truth tables features the same larger state space problem, we adapt AlphaZero’s effective search and pruning capabilities to navigate AIG generation. By combining a policy module to propose actions and a value module to evaluate state viability, AlphaZero uses selection strategy that strikes a balance between exploitation and exploration. The selection strategy, predictor upper confidence bound applied to trees (PUCT) used by AlphaZero, is defined as:

$$\text{PUCT}(s, a) = Q(s, a) + cP(s, a) \frac{\sqrt{\sum_a N(s, a)}}{N(s, a) + 1}$$

where, $Q(s, a)$ represents the expected Q-value, $P(s, a)$ is the policy module’s probability distribution, $N(s, a)$ tracks state visitations, and c is a parameter to balance exploitation and exploration. Computing $Q(s_t, a)$ for every action is too expensive, so we initialize $Q(s_t, a) = 0$, perform the action that maximizes $\text{PUCT}(s_t, a)$, and only compute the value of the state $Q(s_{t+1})$ once we visit it. The term $Q(s, a)$ represents the exploitation in PUCT, as if during search our method discovers a “good” state, we exploit it and focus the search locally to discover more compact designs. The term $P(s, a)$ suggests actions to perform, but the term $\sqrt{\sum_a N(s, a)}/(N(s, a)+1)$ promotes exploration. Additionally, AlphaZero injects Dirichlet noise into the $P(s, a)$ of the root node to promote further exploration.

AlphaZero stores intermediate results and useful metadata, such as $Q(s, a)$, $P(s, a)$, and $N(s, a)$, in the nodes visited during MCTS. These nodes are associated with a state and form a tree, where edges indicate the action performed to reach that node-state pair. When the simulation phase starts, we mark the initial state as the root node, compute the probability action distribution, and inject Dirichlet noise. During a simulation, AlphaZero selects an action according to PUCT and visits the state. This process continues until one of the three stopping conditions, which are encountering a state s that has not been expanded, reaching the maximum number of allowed steps, or arriving at a terminal state. If the state is not expanded yet, it means we have not computed $Q(s)$ and $P(s, a)$ for that state. After computing these values, we back-propagate the Q-value $Q(s)$ to the previous MCTS nodes and increment $N(s, a)$ for all visited nodes. Once we complete the given number of simulations, AlphaZero performs the action it most often selected at the root, $\text{argmax}_{a \in \mathcal{A}} N(s, a)$.

In our case, we can also utilize AlphaZero formulation without relying on the value module. Instead of stopping the simulation when a non-expanded node is encountered, we continue until either we reach the maximum number of steps or if we find a terminal state. When we obtain a terminal reward, we back-propagate it to the intermediate states, enabling exploitation of these states in subsequent simulations while also allowing local exploration to potentially uncover more compact solutions.

5.2.2 FINE-TUNING FLOW

Generating trajectories for millions of truth tables is challenging. Thus, to maximize computational resources, our fine-tuning regimen consists of data collection and model training processes. These processes generate trajectories and add their findings to a replay buffer of fixed length. Simultaneously, we run a few distributed model training processes on GPU that consume data from the replay

buffer. After a fixed number of training steps, the training processes broadcast the model’s updated weights to the data collection processes, and a new epoch starts. Under the hood, the data collection processes store metadata of the MCTS root node for each step in the trajectory in the replay buffer. Specifically, this includes all truth tables of the nodes and the target, the visitation count $N(s, a)$, and the score assigned to the state $Q(s)$.

Training processes randomly sample data from the replay buffer uses the truth tables of the nodes and the target as input for the model. Since the value module aims to predict the Q-value of a state, the goal in this phase is to minimize the mean squared error (MSE) between the predicted value and the retrieved $Q(s)$. Finally, the target distribution for the policy module is the normalized number of visitations $N(s,a)/\sum_a N(s,a)$. Similar to pre-training, we minimize the KL-divergence between the output of the policy module and the target probability distribution. Note that during fine-tuning, the target probability distribution shifts and becomes more aligned with the perspective of the value module, since visitation occurs according to PUCT, which also depends on the value module’s predictions.

6 EXPERIMENTAL EVALUATION

We introduce the implementation details such as model and search hyperparameters, datasets and baseline methods in section 6.1. We compare the effectiveness of ShortCircuit against several baselines in 6.3 compares. Finally, section 6.4 presents an ablation study to demonstrate the effectiveness of the different components within our method.

6.1 EXPERIMENTAL SETUP

We train and evaluate ShortCircuit on the 8-input truth tables that we randomly extract from the EPFL benchmark as described in section 5.1.1. We specifically choose to test on these circuits, since they correspond to real-world Boolean functions that have more practical interest than uniformly random truth-tables. In total, we extract 1.8 million AIGs with an average number of AND-nodes of 10.08.

We train ShortCircuit on a server with an Intel(R) Xeon(R) Platinum 8462Y+ CPU with 500GB RAM and 4x Nvidia L40 with 46GB VRAM each. It takes about four days to pre-train our model for 400 epochs with a batch size of 1024. We use a cosine annealing with warm restarts learning rate scheduler with a starting learning rate of 1×10^{-3} , and we clip the gradients to 1.0. Our transformer blocks follow the structure of Llama 3 (Meta Llama team, 2024), and the number of transformer blocks we use are $P = H = S = 2$ as depicted in Figure 2. With 16 heads and an intermediate embedding size of 4096, our model comprises almost 35 million parameters. During pre-training, we apply a uniformly sampled permutation transform to the training sequences with probability 75%, and a target negation transform with probability 50%. Finally, to speed-up pre-training, we use a distributed dataloader yielding batches of sequences of same length to avoid applying padding and consequently unnecessary computations.

6.2 BASELINES

Each truth table in our test set is built from the primary output of an extracted cut. Therefore, given a test truth table computed from a given cut, we use this cut as a baseline, denoted as `Cut`, as it is an AIG realising the target truth table. While generating correct AIGs is already a challenging task for a neural network, we strive to create near-optimal graphs. Although determining the optimality of an AIG is not computationally tractable, we can leverage a popular logic optimization flow, `resyn2`, which applies multiple operators to optimize AIG size. While `resyn2` cannot guarantee the optimality of the resulting AIG, it provides a reliable proxy for optimality at the current graph sizes, which we represent as a horizontal line with the tick label **O**, when applicable. Additionally, we compare ShortCircuit against the state-of-the-art open-source logic synthesis tool `ABC`. This library generates an AIG by applying a series of Boolean algebra transformations, converting the truth table into a Binary Decision Diagram (BDD), then to a Sum of Products (SoP), and finally to an AIG. The sequence of commands we use to generate an AIG with `ABC` is as follows: `read_truth -x [truth table]; collapse; sop; strash; write [outfile]`.

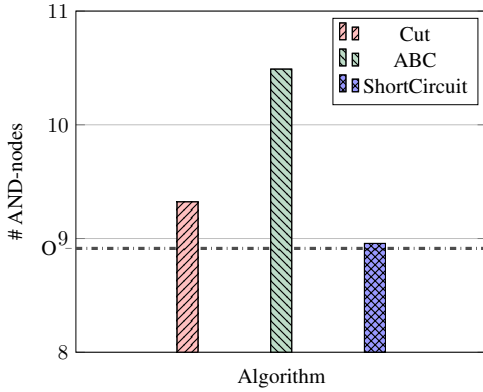


Figure 4: Average number of AND-nodes for the successfully generated across different methods. The `Cut` baseline corresponds to the AIGs extracted from larger circuits, `ABC` leverages formal Boolean methods to generate an AIG, and `ShortCircuit` utilizes purely Machine Learning. The dashed horizontal line indicates the average optimal size of those AIGs.

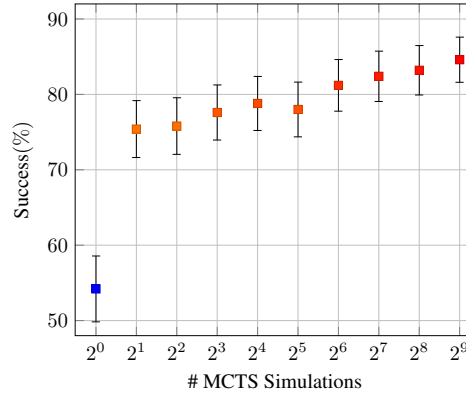


Figure 5: Success rate of `ShortCircuit` in generating correct AIGs when it performs actions in a 1-512 MCTS simulations before per performing an action.

6.3 GENERATION QUALITY EXPERIMENTS

We evaluate `ShortCircuit` against the baseline methods on 500 truth tables associated with randomly sampled AIGs from the EPFL benchmark suite. The success rate of `ShortCircuit` on this test set is 84.6%. In this version, `ShortCircuit` relies solely on its policy module, and we allow `ShortCircuit` to attempt to generate a circuit with up to 30 AND-nodes. Before deciding which AND-node to generate, `ShortCircuit` performs 512 MCTS simulations, generating up to 20 AND-nodes in each simulation. Figure 4 compares the average number of AND-nodes for the successfully generated circuits against the baselines `Cut` and `ABC`. `ShortCircuit` generates very compact AIGs, near-optimal as indicated by the horizontal line at the tick **O**. Specifically, `ShortCircuit` produces circuits with 8.96 AND-nodes on average, which is 0.49% larger than the optimal ones that have 8.91 AND-nodes on average. Furthermore, the AIGs generated by `ShortCircuit` are significantly smaller than the ones from the baselines `Cut` and `ABC`, which respectively contain 9.32 and 10.49 AND-nodes, corresponding to a relative size reduction with `ShortCircuit` of 3.93% and 14.61%, respectively. The average time to generate an AIG is 128.7s which depends on how fast a solution can be discovered. While these results demonstrate the effectiveness of `ShortCircuit`, different parameters, such as a larger number of AND-node limits, can further improve the success rate, albeit at the cost of an increased running time.

6.4 ABLATION STUDY

To better understand the role of MCTS simulations in the performance of `ShortCircuit`, we conduct an ablation study to investigate their impact on the success rate, the circuit size, and the execution time. Using the same test set of 500 truth tables as in section 6.3, we evaluate our method’s performance when it solely relies on its policy module. Figure 5 illustrates how the success rate evolves as the number of MCTS simulations increases from 1 to 512. For clarity, we append an integer i next to our method’s name (`ShortCircuit`[i]) to indicate the number of simulations we perform.

When using only 1 simulation, `ShortCircuit`[1] performs a greedy search, where the policy selects the most probable action, $a = \operatorname{argmax}_{a \in \mathcal{A}} P(s, a)$. This greedy strategy yields a low success rate of 54.2% but benefits from a very short generation time of just 0.08s. On the other end, `ShortCircuit`[512] achieves a significantly higher success rate of 84.6%, albeit with a much longer running time of 128.75s. Interestingly, while increasing the number of MCTS simulations generally improves performance, `ShortCircuit`[512] does not consistently outperform all versions with fewer

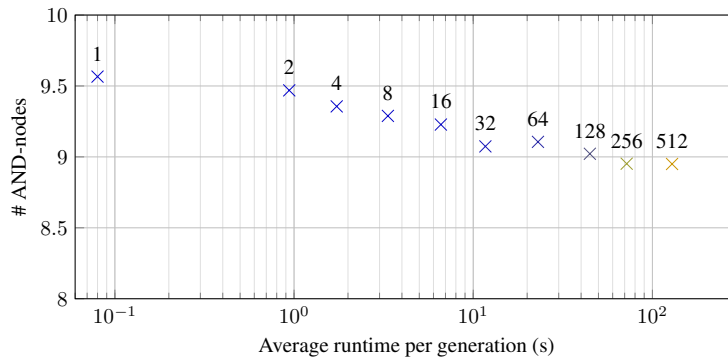


Figure 6: Average number of AND-nodes for the successfully generated AIGs and running time per generation when we vary the number of MCTS simulations ShortCircuit performs. The number of simulations is on top of each data point

simulations. In fact, when aggregating the successfully generated AIGs across all settings, ShortCircuit achieves a total success rate of 92.2%.

Increasing the number of simulations enables the model to explore a larger – but still limited – portion of the solution space, resulting in higher success rates and the discovery of more compact circuit designs. While this improves the overall success rate, as shown earlier, it also comes with the trade-off of increased execution time. Figure 6 highlights this trade-off by revealing a Pareto front, suggesting that we can adjust the number of MCTS simulations to achieve the desired balance between success rate, design quality, and execution time.

7 CONCLUSION

In this paper, we introduced ShortCircuit, a novel transformer-based architecture designed to generate AIGs from target truth tables. Our approach combines a structurally aware transformer model with an AlphaZero-inspired policy variant, enabling efficient navigation through the doubly exponential state space associated with truth tables. Through extensive experiments, we demonstrated the effectiveness of ShortCircuit in producing high-quality AIGs that are significantly smaller than those generated by one of the state-of-the-art logic synthesis tools. Specifically, our method achieved a relative size reduction of 3.93% and 14.61% compared to the baselines Cut and ABC, respectively.

This work contributes to the expanding field of machine learning applications in chip design, showcasing the potential of deep learning techniques to revitalize the field with new perspectives. By harnessing the power of transformer models and the strategic search capabilities of AlphaZero, we demonstrated that it is possible to generate high-quality AIGs from truth tables, paving the way for future research in this area. Future work will focus on extending ShortCircuit to handle AIGs with multiple outputs, integrating our approach with existing logic synthesis tools, exploring its application in industrial settings. Finally, our goal is to enable the creation of more efficient, scalable, and innovative computing systems, and we believe that ShortCircuit is an important step towards realizing this vision.

REFERENCES

- Alan Mishchenko and Robert K. Brayton. Scalable logic synthesis using a simple circuit structure. 2006. URL <https://api.semanticscholar.org/CorpusID:8597391>.
- Clifford Wolf, Johann Glaser, and Johannes Kepler. Yosys-a free verilog synthesis suite. 2013. URL <https://api.semanticscholar.org/CorpusID:202611483>.
- Alan Mishchenko et al. Abc: A system for sequential synthesis and verification. URL <http://www.eecs.berkeley.edu/alanmi/abc>, 17, 2007.

- Peter A. Beerel and Massoud Pedram. Opportunities for machine learning in electronic design automation. In *2018 IEEE International Symposium on Circuits and Systems (ISCAS)*, pages 1–5, 2018. doi: 10.1109/ISCAS.2018.8351731.
- Guyue Huang, Jingbo Hu, Yifan He, Jialong Liu, Mingyuan Ma, Zhaoyang Shen, Juejian Wu, Yuanfan Xu, Hengrui Zhang, Kai Zhong, Xuefei Ning, Yuzhe Ma, Haoyu Yang, Bei Yu, Huazhong Yang, and Yu Wang. Machine learning for electronic design automation: A survey. *ACM Trans. Design Autom. Electr. Syst.*, 26:40:1–40:46, 2021. URL <https://api.semanticscholar.org/CorpusID:231839647>.
- Kevin Immanuel Gubbi, Sayed Aresh Beheshti-Shirazi, Tyler Sheaves, Soheil Salehi, Sai Manoj PD, Setareh Rafatirad, Avesta Sasan, and Houman Homayoun. Survey of machine learning for electronic design automation. In *Proceedings of the Great Lakes Symposium on VLSI 2022, GLSVLSI '22*, page 513–518, New York, NY, USA, 2022. Association for Computing Machinery. ISBN 9781450393225. doi: 10.1145/3526241.3530834. URL <https://doi.org/10.1145/3526241.3530834>.
- Samuel I. Ward, Myung-Chul Kim, Natarajan Viswanathan, Zhuo Li, Charles J. Alpert, Earl E. Swartzlander, and David Z. Pan. Keep it straight: teaching placement how to better handle designs with datapaths. In *ACM International Symposium on Physical Design, 2012a*. URL <https://api.semanticscholar.org/CorpusID:8570378>.
- Samuel Ward, Duo Ding, and David Z. Pan. Pade: A high-performance placer with automatic datapath extraction and evaluation through high-dimensional data learning. In *DAC Design Automation Conference 2012*, pages 756–761, 2012b. doi: 10.1145/2228360.2228497.
- Zhiyao Xie, Yu-Hung Huang, Guan-Qi Fang, Haoxing Ren, Shao-Yun Fang, Yiran Chen, and Jiang Hu. Routenet: Routability prediction for mixed-size designs using convolutional neural network. In *2018 IEEE/ACM International Conference on Computer-Aided Design (ICCAD)*, pages 1–8, 2018. doi: 10.1145/3240765.3240843.
- Mohamed Baker Alawieh, Wuxi Li, Yibo Lin, Love Singhal, Mahesh A. Iyer, and David Z. Pan. High-definition routing congestion prediction for large-scale fpgas. In *2020 25th Asia and South Pacific Design Automation Conference (ASP-DAC)*, pages 26–31, 2020. doi: 10.1109/ASP-DAC47756.2020.9045178.
- Shai Fine and Avi Ziv. Coverage directed test generation for functional verification using bayesian networks. In *Proceedings of the 40th Annual Design Automation Conference, DAC '03*, page 286–291, New York, NY, USA, 2003. Association for Computing Machinery. ISBN 1581136889. doi: 10.1145/775832.775907. URL <https://doi.org/10.1145/775832.775907>.
- Ilya Wagner, Valeria Bertacco, and Todd Austin. Microprocessor verification via feedback-adjusted markov models. *IEEE Transactions on Computer-Aided Design of Integrated Circuits and Systems*, 26(6):1126–1138, 2007. doi: 10.1109/TCAD.2006.884494.
- Kaihui Tu, Xifan Tang, Cunxi Yu, Lana Josipović, and Zhufei Chu. *Logic Synthesis*, pages 135–164. Springer Nature Singapore, Singapore, 2024. ISBN 978-981-99-7755-0. doi: 10.1007/978-981-99-7755-0_9. URL https://doi.org/10.1007/978-981-99-7755-0_9.
- Winston Haaswijk, Edo Collins, Benoit Seguin, Mathias Soeken, Frédéric Kaplan, Sabine Süsstrunk, and Giovanni De Micheli. Deep learning for logic optimization algorithms. In *2018 IEEE International Symposium on Circuits and Systems (ISCAS)*, pages 1–4, 2018a. doi: 10.1109/ISCAS.2018.8351885.
- Cunxi Yu, Houping Xiao, and Giovanni De Micheli. Developing synthesis flows without human knowledge. In *Proceedings of the 55th Annual Design Automation Conference, DAC '18*, New York, NY, USA, 2018. Association for Computing Machinery. ISBN 9781450357005. doi: 10.1145/3195970.3196026. URL <https://doi.org/10.1145/3195970.3196026>.
- Abdelrahman Hosny, Soheil Hashemi, Mohamed Shalan, and Sherief Reda. DRiLLS: Deep Reinforcement Learning for Logic Synthesis. *2020 25th Asia and South Pacific Design Automation Conference (ASP-DAC)*, pages 581–586, September 2020. doi: 10.1109/ASP-DAC47756.2020.9045559.

- Jianyong Yuan, Peiyu Wang, Junjie Ye, Mingxuan Yuan, Jianye Hao, and Junchi Yan. Easyso: Exploration-enhanced reinforcement learning for logic synthesis sequence optimization and a comprehensive rl environment. *2023 IEEE/ACM International Conference on Computer Aided Design (ICCAD)*, pages 1–9, 2023. URL <https://api.semanticscholar.org/CorpusID:265526066>.
- Keren Zhu, Mingjie Liu, Hao Chen, Zheng Zhao, and David Z. Pan. Exploring logic optimizations with reinforcement learning and graph convolutional network. In *Proceedings of the 2020 ACM/IEEE Workshop on Machine Learning for CAD, MLCAD '20*, page 145–150, New York, NY, USA, 2020a. Association for Computing Machinery. ISBN 9781450375191. doi: 10.1145/3380446.3430622. URL <https://doi.org/10.1145/3380446.3430622>.
- Yu Qian, Xuegong Zhou, Hao Zhou, and Lingli Wang. An efficient reinforcement learning based framework for exploring logic synthesis. *ACM Trans. Des. Autom. Electron. Syst.*, 29(2), jan 2024. ISSN 1084-4309. doi: 10.1145/3632174. URL <https://doi.org/10.1145/3632174>.
- Animesh Basak Chowdhury, Marco Romanelli, Benjamin Tan, Ramesh Karri, and Siddharth Garg. Retrieval-guided reinforcement learning for boolean circuit minimization. In *The Twelfth International Conference on Learning Representations*, 2024. URL <https://openreview.net/forum?id=0t108ziRZp>.
- Zehua Pei, Fangzhou Liu, Zhuolun He, Guojin Chen, Haisheng Zheng, Keren Zhu, and Bei Yu. Alphasyn: Logic synthesis optimization with efficient monte carlo tree search. In *2023 IEEE/ACM International Conference on Computer Aided Design (ICCAD)*, pages 1–9, 2023. doi: 10.1109/ICCAD57390.2023.10323856.
- Antoine Grosnit, Cedric Malherbe, Rasul Tutunov, Xingchen Wan, Jun Wang, and Haitham Bou Ammar. Boils: Bayesian optimisation for logic synthesis. In *2022 Design, Automation & Test in Europe Conference & Exhibition (DATE)*, pages 1193–1196. IEEE, 2022.
- Chang Feng, Wenlong Lyu, Zhitang Chen, Junjie Ye, Min jie Yuan, and Jianye Hao. Batch sequential black-box optimization with embedding alignment cells for logic synthesis. *2022 IEEE/ACM International Conference On Computer Aided Design (ICCAD)*, pages 1–9, 2022. URL <https://api.semanticscholar.org/CorpusID:254927570>.
- Stéphane d’Ascoli, Samy Bengio, Joshua M. Susskind, and Emmanuel Abbe. Boolformer: Symbolic regression of logic functions with transformers, 2024. URL <https://openreview.net/forum?id=wmzFZ91JrD>.
- Xihan Li, Xing Li, Lei Chen, Xing Zhang, Mingxuan Yuan, and Jun Wang. Circuit transformer: End-to-end circuit design by predicting the next gate. *ArXiv*, abs/2403.13838, 2024a. URL <https://api.semanticscholar.org/CorpusID:268553512>.
- Xihan Li, Xing Li, Lei Chen, Xing Zhang, Mingxuan Yuan, and Jun Wang. Logic synthesis with generative deep neural networks. *ArXiv*, abs/2406.04699, 2024b. URL <https://api.semanticscholar.org/CorpusID:270357641>.
- Yao Lai, Sungyoung Lee, Guojin Chen, Souradip Poddar, Mengkang Hu, David Z. Pan, and Ping Luo. Analogcoder: Analog circuit design via training-free code generation. *ArXiv*, abs/2405.14918, 2024. URL <https://api.semanticscholar.org/CorpusID:270045319>.
- Zehao Dong, Weidong Cao, Muhan Zhang, Dacheng Tao, Yixin Chen, and Xuan Zhang. Cktgnn: Circuit graph neural network for electronic design automation. *arXiv preprint arXiv:2308.16406*, 2023.
- David Silver, Aja Huang, Chris J. Maddison, Arthur Guez, Laurent Sifre, George van den Driessche, Julian Schrittwieser, Ioannis Antonoglou, Vedavyas Panneershelvam, Marc Lanctot, Sander Dieleman, Dominik Grewe, John Nham, Nal Kalchbrenner, Ilya Sutskever, Timothy P. Lillicrap, Madeleine Leach, Koray Kavukcuoglu, Thore Graepel, and Demis Hassabis. Mastering the game of go with deep neural networks and tree search. *Nat.*, 529(7587):484–489, 2016. doi: 10.1038/NATURE16961. URL <https://doi.org/10.1038/nature16961>.

- David Silver, Thomas Hubert, Julian Schrittwieser, Ioannis Antonoglou, Matthew Lai, Arthur Guez, Marc Lanctot, Laurent Sifre, Dhharshan Kumaran, Thore Graepel, Timothy P. Lillicrap, Karen Simonyan, and Demis Hassabis. Mastering chess and shogi by self-play with a general reinforcement learning algorithm. *CoRR*, abs/1712.01815, 2017. URL <http://arxiv.org/abs/1712.01815>.
- John M. Jumper, Richard Evans, Alexander Pritzel, Tim Green, Michael Figurnov, Olaf Ronneberger, Kathryn Tunyasuvunakool, Russ Bates, Augustin Žídek, Anna Potapenko, Alex Bridgland, Clemens Meyer, Simon A A Kohl, Andy Ballard, Andrew Cowie, Bernardino Romera-Paredes, Stanislav Nikolov, Rishub Jain, Jonas Adler, Trevor Back, Stig Petersen, David Reiman, Ellen Clancy, Michal Zielinski, Martin Steinegger, Michalina Pacholska, Tamas Berghammer, Sebastian Bodenstein, David Silver, Oriol Vinyals, Andrew W. Senior, Koray Kavukcuoglu, Pushmeet Kohli, and Demis Hassabis. Highly accurate protein structure prediction with alphafold. *Nature*, 596:583 – 589, 2021. URL <https://api.semanticscholar.org/CorpusID:235959867>.
- Jacob Devlin, Ming-Wei Chang, Kenton Lee, and Kristina Toutanova. Bert: Pre-training of deep bidirectional transformers for language understanding. In *North American Chapter of the Association for Computational Linguistics*, 2019. URL <https://api.semanticscholar.org/CorpusID:52967399>.
- Jared Kaplan, Sam McCandlish, Tom Henighan, Tom B. Brown, Benjamin Chess, Rewon Child, Scott Gray, Alec Radford, Jeff Wu, and Dario Amodei. Scaling laws for neural language models. *ArXiv*, abs/2001.08361, 2020. URL <https://api.semanticscholar.org/CorpusID:210861095>.
- Tom B. Brown, Benjamin Mann, Nick Ryder, Melanie Subbiah, Jared Kaplan, Prafulla Dhariwal, Arvind Neelakantan, Pranav Shyam, Girish Sastry, Amanda Askell, Sandhini Agarwal, Ariel Herbert-Voss, Gretchen Krueger, Tom Henighan, Rewon Child, Aditya Ramesh, Daniel M. Ziegler, Jeff Wu, Clemens Winter, Christopher Hesse, Mark Chen, Eric Sigler, Ma teusz Litwin, Scott Gray, Benjamin Chess, Jack Clark, Christopher Berner, Sam McCandlish, Alec Radford, Ilya Sutskever, and Dario Amodei. Language models are few-shot learners. *ArXiv*, abs/2005.14165, 2020. URL <https://api.semanticscholar.org/CorpusID:218971783>.
- Maurice Karnaugh. The map method for synthesis of combinational logic circuits. *Transactions of the American Institute of Electrical Engineers, Part I: Communication and Electronics*, 72: 593–599, 1953. URL <https://api.semanticscholar.org/CorpusID:51636736>.
- W. V. Quine. The problem of simplifying truth functions. *The American Mathematical Monthly*, 59(8):521–531, 1952. ISSN 00029890, 19300972. URL <http://www.jstor.org/stable/2308219>.
- W. V. Quine. A way to simplify truth functions. *The American Mathematical Monthly*, 62(9):627–631, 1955. ISSN 00029890, 19300972. URL <http://www.jstor.org/stable/2307285>.
- E. J. McCluskey Jr. Minimization of boolean functions. *Bell System Technical Journal*, 35(6):1417–1444, 1956. doi: <https://doi.org/10.1002/j.1538-7305.1956.tb03835.x>. URL <https://onlinelibrary.wiley.com/doi/abs/10.1002/j.1538-7305.1956.tb03835.x>.
- R.L. Rudell and A. Sangiovanni-Vincentelli. Multiple-valued minimization for pla optimization. *IEEE Transactions on Computer-Aided Design of Integrated Circuits and Systems*, 6(5):727–750, 1987. doi: 10.1109/TCAD.1987.1270318.
- Alan Mishchenko, Robert Brayton, Stephen Jang, and Victor Kravets. Delay optimization using sop balancing. In *2011 IEEE/ACM International Conference on Computer-Aided Design (ICCAD)*, pages 375–382, 2011. doi: 10.1109/ICCAD.2011.6105357.
- John A. Darringer, William H. Joyner, C. Leonard Berman, and Louise Trevillyan. Logic synthesis through local transformations. *IBM Journal of Research and Development*, 25(4):272–280, 1981. doi: 10.1147/rd.254.0272.

- Alan Mishchenko, Satrajit Chatterjee, and Robert Brayton. Dag-aware aig rewriting a fresh look at combinational logic synthesis. In *Proceedings of the 43rd Annual Design Automation Conference, DAC '06*, page 532–535, New York, NY, USA, 2006. Association for Computing Machinery. ISBN 1595933816. doi: 10.1145/1146909.1147048. URL <https://doi.org/10.1145/1146909.1147048>.
- Heinz Riener, Eleonora Testa, Winston Haaswijk, Alan Mishchenko, Luca Amarù, Giovanni De Micheli, and Mathias Soeken. Scalable generic logic synthesis: One approach to rule them all. In *2019 56th ACM/IEEE Design Automation Conference (DAC)*, pages 1–6, 2019.
- Guanglei Zhou and Jason H. Anderson. Area-driven fpga logic synthesis using reinforcement learning. In *2023 28th Asia and South Pacific Design Automation Conference (ASP-DAC)*, pages 159–165, 2023.
- Winston Haaswijk, Edo Collins, Benoit Seguin, Mathias Soeken, Frédéric Kaplan, Sabine Süssstrunk, and Giovanni De Micheli. Deep learning for logic optimization algorithms. In *2018 IEEE International Symposium on Circuits and Systems (ISCAS)*, pages 1–4, 2018b. doi: 10.1109/ISCAS.2018.8351885.
- Keren Zhu, Mingjie Liu, Hao Chen, Zheng Zhao, and David Z. Pan. Exploring logic optimizations with reinforcement learning and graph convolutional network. In *2020 ACM/IEEE 2nd Workshop on Machine Learning for CAD (MLCAD)*, pages 145–150, 2020b. doi: 10.1145/3380446.3430622.
- Yasasvi V. Peruvemba, Shubham Rai, Kapil Ahuja, and Akash Kumar. RI-guided runtime-constrained heuristic exploration for logic synthesis. In *2021 IEEE/ACM International Conference On Computer Aided Design (ICCAD)*, page 1–9. IEEE Press, 2021. doi: 10.1109/ICCAD51958.2021.9643530. URL <https://doi.org/10.1109/ICCAD51958.2021.9643530>.
- Animesh Basak Chowdhury, Benjamin Tan, Ryan Carey, Tushit Jain, Ramesh Karri, and Sidharth Garg. Bulls-eye: Active few-shot learning guided logic synthesis. *IEEE Transactions on Computer-Aided Design of Integrated Circuits and Systems*, 42(8):2580–2590, 2023. doi: 10.1109/TCAD.2022.3226668.
- Cunxi Yu and Wang Zhou. Decision making in synthesis cross technologies using lstms and transfer learning. In *2020 ACM/IEEE 2nd Workshop on Machine Learning for CAD (MLCAD)*, pages 55–60, 2020. doi: 10.1145/3380446.3430638.
- Nan Wu, Jiwon Lee, Yuan Xie, and Cong Hao. Lostin: Logic optimization via spatio-temporal information with hybrid graph models. In *2022 IEEE 33rd International Conference on Application-specific Systems, Architectures and Processors (ASAP)*, pages 11–18, 2022. doi: 10.1109/ASAP54787.2022.00013.
- Peter Belcak and Roger Wattenhofer. Neural combinatorial logic circuit synthesis from input-output examples. *CoRR*, abs/2210.16606, 2022. doi: 10.48550/ARXIV.2210.16606. URL <https://doi.org/10.48550/arXiv.2210.16606>.
- Matthieu Zimmer, Xuening Feng, Claire Glanois, Zhaohui JIANG, Jianyi Zhang, Paul Weng, Dong Li, Jianye HAO, and Wulong Liu. Differentiable logic machines. *Transactions on Machine Learning Research*, 2023. ISSN 2835-8856. URL <https://openreview.net/forum?id=mXfkKtu5JA>.
- Adam Hillier, Ngân (NV) Vũ, Daniel J. Mankowitz, Daniele Calandriello, Edouard Leurent, Georges Rotival, Ivan Lobov, Kshiteej Mahajan, Marco Gelmi, and Natasha Antropova. Learning to design efficient logic circuits, 2023. URL <https://cassyni.com/events/S2LPTWZeMh9TGcLJe5jppqK>. NANDA Workshop 2023.
- Rajarshi Roy, Jonathan Raiman, Neel Kant, Ilyas Elkin, Robert Kirby, Michael Siu, Stuart Oberman, Saad Godil, and Bryan Catanzaro. Prefixrl: Optimization of parallel prefix circuits using deep reinforcement learning. In *2021 58th ACM/IEEE Design Automation Conference (DAC)*, pages 853–858, 2021. doi: 10.1109/DAC18074.2021.9586094.

Mufei Li, Viraj Shitole, Eli Chien, Changhai Man, Zhaodong Wang, Srinivas, Ying Zhang, Tushar Krishna, and Pan Li. LayerDAG: A layerwise autoregressive diffusion model of directed acyclic graphs for system. In *Machine Learning for Computer Architecture and Systems 2024*, 2024c. URL <https://openreview.net/forum?id=IsarrieQA>.

Luca Amarú, Pierre-Emmanuel Gaillardon, and Giovanni De Micheli. The epfl combinational benchmark suite. In *Proceedings of the 24th International Workshop on Logic & Synthesis (IWLS)*, number CONF, 2015.

Meta Llama team. Introducing meta llama 3: The most capable openly available llm to date. *Meta AI Blog*, 2024. URL <https://ai.meta.com/blog/meta-llama-3/>.

A NOTATIONS

Table 3 contains a condensed summary of the notation introduced throughout the paper.

Symbol	Meaning
n	Number of inputs in the AIG
I_j	Input node j in the AIG
O	Output node for the AIG
\wedge_i	AND-node i for the AIG
T_*	Target truth table
s	State
a	Action
\mathcal{T}	Set of truth tables in the AIG
\mathcal{A}	Set of actions
N	Current number of nodes in the AIG
N_{\max}	Max number of nodes allowed in the AIG ShortCircuit generates
ϵ	Building type of an AND-node with respect to its two fanins (Table 2)
\mathbf{A}	Sparse 3-dimensional tensor accumulating all the target actions
\mathbb{S}_k	Set of permutations of $\{1..k\}$
$\sigma(\cdot)$	Random row permutation function
$Q(s, a)$	Expected Q-value for a state s and action a
$P(s, a)$	Probability distribution
$N(s, a)$	Visit count of action a and state s
c	Parameter balancing exploration and exploitation in PUCT

Table 3: List of symbols and notations used in the paper.

B DATA COLLECTION

B.1 EPFL BENCHMARKS

Tables 4 and 5, contain detailed information about the arithmetic and random control circuits in the EPFL benchmarks (Amarú et al., 2015), respectively. The circuits have been mapped from behavioral descriptions into logic gates and are intentionally suboptimal for scientific purposes. Arithmetic circuits, as their name hints, are combinatorial AIGs representing an arithmetic operation such as square root, logarithm, etc., while the set of random control circuits consists of controller circuits.

Circuit Name	# Inputs	# Outputs	# AND-nodes	Levels
Adder	256	129	1020	255
Barrel Shifter	135	128	3336	12
Divisor	128	128	44762	4470
Hypotenuse	256	128	214335	24801
Log2	32	32	32060	444
Max	512	130	2865	287
Multiplier	128	128	27062	274
Sine	24	25	5416	225
Square-root	128	64	24618	5058
Square	64	128	18484	250

Table 4: Arithmetic circuits in the EPFL benchmark suite and their statistics

B.2 CUT EXTRACTION

To extract a cut from a given node with a target number of inputs n , we designate the given node as the root and of the cut and its two parents as the initial leaf set. We then iteratively remove a random

Circuit Name	# Inputs	# Outputs	# AND-nodes	Levels
Round-Robin Arbiter	256	129	11839	87
Alu Control Unit	7	26	174	10
Coding-Cavlc	19	11	693	16
Decoder	8	128	304	3
i2c Controller	147	142	1342	20
Int to Float Converter	11	7	260	16
Memory Controller	1204	1231	46836	114
Priority Encoder	128	8	978	250
Lookahead XY Router	60	30	257	54
Voter	1001	1	13758	70

Table 5: Random/Control circuits in the EPFL benchmark suite and their statistics

node from the leaf set and add its parents to the leaf set while maintaining the leaf property. This process continues until the leaf set contains n nodes. Finally, we create an AIG out of the visited nodes within the cut where we mark the leaf set as the inputs and the root node as the output. We provide the outline of the procedure in Algorithm 1.

Algorithm 1 Cut Extraction

Require: Root node: r , number of cut inputs: n

- 1: leaf_set = {left_parent(r), right_parent(r)}
 - 2: node_set = { r }
 - 3: **while** size(leaf_set) < n **do**
 - 4: node = leaf_set.random_pop()
 - 5: node_set.insert(node)
 - 6: leaf_set.insert(left_parent(node)) & leaf_set.insert(right_parent(node))
 - 7: Ensure leaf property in leaf_set
 - 8: Construct AIG from leaf_set and node_set
-

We can modify this algorithm to extract additional cuts per node by repeating the process until we find a cut with $n - 1$ leaf nodes. For this cut, instead of randomly expanding a leaf node, we create $n - 1$ copies of the cut and expand each leaf node individually, storing the resulting cuts. In practice, we actually employ Algorithm 2 to extract AIGs from the EPFL circuits. Although Algorithm 1 conveys the core idea of AIG extraction, the following algorithm is more effective from an engineering standpoint, as it allows to extract more cuts from the same node.

The revised algorithm takes two inputs: n , the desired number of input nodes, and the root node. It initializes the leaf set by adding the parents of the root node. It then iteratively removes a random node from the leaf set and expands it using Algorithm 3. This process continues until the cut contains $n - 1$ leaf nodes, at which point we create $n - 1$ copies of the current cut state and expand each leaf node to generate n unique cuts. For brevity, we omitted the details of ensuring the leaf property after node expansion in the main text, which is addressed in Algorithm 4. This algorithm ensures that no node in the leaf set has a parent also in this set, which would violate the leaf property. If a parent is already in the leaf set, we can remove the node from the set and add the other parent that is not yet in the leaf set.

Algorithm 2 Multi-Cut Extraction

Require: Root node: r , Number of cut inputs: n

- 1: leaf_set = {left_parent(r), right_parent(r)}
- 2: node_set = { r }
- 3: **while** size(leaf_set) < $n - 1$ **do**
- 4: node = leaf_set.random_pop()
- 5: Cut_Expansion(node, leaf_set, node_set)
- 6: **for** leaf in leaf_set **do**
- 7: copy_leaf_set = leaf_set.copy() & copy_node_set = node_set.copy()
- 8: copy_leaf_set.delete(leaf)
- 9: Cut_Expansion(leaf, copy_leaf_set, copy_node_set)
- 10: Construct AIG from copy_leaf_set and copy_node_set

Algorithm 3 Cut Expansion

Require: Node to expand: node, Current leaf nodes: leaf_set, Current nodes in cut: node_set

- 1: node_set.insert(node)
- 2: leaf_set.insert(left_parent(node)) & leaf_set.insert(right_parent(node))
- 3: preserve_leaf_property(leaf_set, node_set)

Algorithm 4 Preserve Leaf Property

Require: Current leaf nodes: leaf_set, Current nodes in cut: node_set

- 1: **for** leaf in leaf_set **do**
- 2: **if** left_parent(leaf) in leaf_set **then**
- 3: leaf_set.delete(leaf) & node_set.insert(leaf)
- 4: leaf_set.insert(right_parent(leaf))
- 5: **else if** right_parent(leaf) in leaf_set **then**
- 6: leaf_set.delete(leaf) & node_set.insert(leaf)
- 7: leaf_set.insert(left_parent(leaf))
